Manuscript submitted to **Biophysical***Journal*

Article

Glucocerebrosidase rescues alpha-synuclein from amyloid formation

M.S. Barber[1], H.M. Muller[1], R.G. Gilbert[2], and A.J. Baldwin[1,*]

ABSTRACT Aggregation of the protein α-synuclein (αSyn) into amyloid fibrils is associated with Parkinson's disease (PD), a process accelerated by lipids. Recently, the lysosomal protein glucocerebrosidase (GCase) has been identified as a major risk factor in both genetic and sporadic PD. Here, we use solution state NMR to reveal that GCase directly inhibits lipid induced αSyn amyloidogenesis. Structurally, we show that the mechanism for this requires competition between lipids and GCase for αSyn, binding the N and C termini respectively. The affinity of GCase for the C-terminus of αSyn is such that not only does it inhibit lipid induced amyloid formation, but also it destabilizes mature αSyn amyloid fibrils. These results reveal a competitive molecular "tug-of-war" for αSyn termini by GCase and lipid, providing a mechanistic link between the clinically observed links between changes in GCase abundance and Parkinsons disease.

INTRODUCTION

Parkinson's disease (PD) and other synucleinopathies are a group of neurodegenerative disorders characterized by the aggregation of α-synuclein (αSyn) into amyloid rich bodies known as Lewy Bodies (1). Recent clinical studies have linked PD to the lysosomal lipid lytic enzyme Glucocerebrosidase (GCase). Mutation in GCase is the leading genetic risk factor for PD, with 5-10 % of PD patients carrying one of hundreds of possible GCase mutations (2)(Fig 1A). In sporadic PD, wild type GCase is co-localised with Lewy bodies and depleted in the neuronal cells of the *substantia nigra*, the brain structure associated with PD(3–7). Overall, GCase mutation increases the risk of PD by up to 30 fold (8, 9).

Cellular and animal studies further link GCase to PD. Animal studies of PD demonstrate that knock down of wild type GCase or over expression of mutant GCase causes accumulation of αSyn. Likewise, over expression of wild type GCase can reverse αSyn related pathological and behavioural features in mouse models (10–13). Healthy cells can degrade both αSyn monomers and oligomers through autophagic pathways which culminate in the lysosome (6, 14–17). Lysosomal GCase is depleted in both sporadic and non-sporadic PD (4, 5, 5, 18–24) and intercellular transfer of potentially toxic αSyn oligomers between lysosomes is enhanced by GCase depletion (20, 25, 26). Finally, αSyn has been shown to interact with GCase directly at lysosomal pH to inhibit GCase activity (27, 28). Taken together, these results suggest a molecular relationship between GCase and αSyn that is pertinent to PD. Here we seek to investigate the mechanism by which GCase can rescue αSyn from amyloid formation.

At a molecular level, GCase is a 60 kDa glycoprotein found in the acidic lysosome, where it metabolises glucocerebroside (29). Interestingly, post-translational modifications are vital for GCase activity and stability, and ablation of its four N-linked glycosylation sites leads to an inactive and unstable enzyme (30). Therefore, to understand the interplay between GCase and αSyn, it is necessary to work with human cell derived GCase complete with relevant post-translational modifications (see methods).

The intrinsically disordered αSyn plays a role in synaptic vesicle fusion (31) and forms α-helical arrays on the surface of small unilamellar vesicles (SUVs) (32, 33). The sequence of αSyn can be divided into three distinct regions, an N-terminal lipid binding domain, a central pro-amyloidogenic domain and a C-terminal domain that remains free in the lipid bound form(33, 34).

αSyn aggregates into amyloid fibrils that are characterized by ThT binding, increased β-strand content, and cross-β fibre diffraction patterns (35–38). Notably, this aggregation is accelerated 1000 fold in the presence of membrane mimicking anionic lipids such as DMPS and POPG (32, 39–44), amyloidogenesis is further enhanced in low pH environments (like those found in the lysosome) (45–47). The link between αSyn, GCase, acidity and lipids suggest the lysosome as a likely organelle for the onset of αSyn pathogenesis (6, 11, 14, 15, 17, 20, 23, 26).

To understand how GCase might influence amyloidosis, we here investigate the relationship between lipids, human cell derived, wild-type GCase and full length αSyn under lysosomal conditions by means of solution state nuclear magnetic resonance (NMR) spectroscopy. This technique allows examination of multiple binding partners with transient interactions at atomic resolution. In its protonated form, GCase's relatively high molecular weight would be expected to give unobservably broad resonances. NMR labelling techniques designed to overcome this barrier(48) rely on prokaryotic expression systems which in this case would not provide protein with the required glycan modifications neccessary for study of a physiologically relevant interaction. Building on recent advances(49), we have developed a method for isotope incorporation and assignment of high molecular weight proteins allowing us to characterise human cell-line derived GCase by NMR. ^{1}H-^{15}N HSQC (αSyn) and ^{1}H-^{13}C HMQC (GCase) spectra were recorded over a range of concentrations in the presence and absence of detergent micelles formed from SDS, tween, taurochlorate and physiologically relevant SUVs formed from POPG and DMPS (Fig S1). Phosphatidylserines such as DMPS are found in lysosomal inner leaflets and synaptic vesicles (50, 51). These lipids and detergents cover a range of charges and chain lengths and have been previously used to study αSyn(39–43, 50, 51). By carefully quantifying the data and relating it to binding models with rigorous care to avoid overfitting, we determine the precise mechanism by which lipds, GCase and αSyn interact.

Our NMR results reveal that under lysosomal conditions, GCase and anionic lipids compete for opposite termini of αSyn. The differential affinities of GCase and anionic lipids for the N- and C- termini allow GCase to rescue αSyn from both lipid binding and subsequent amyloid formation. We show that under these conditions, GCase can destabilise mature αSyn fibrils and that αSyn contacts GCase near its active site, providing a structural rationale for GCase inhibition by αSyn. Taken together, these results reveal that under lysosomal conditions, GCase is a potent chaperone, able to inhibit aggregation of αSyn, providing a molecular explanation for its connection to PD.

MATERIALS AND METHODS

Expression and purification of α-synuclein

Human sequence αSyn plasmid was kindly provided by Ad Bax (NIH)(52). Recombinant ^{15}N enriched αSyn was expressed from BL21(DE3) star cells (ThermoFisher, Waltham, Mass.) containing kanamycin resistant, T7, IPTG inducible plasmids (pET 41, Novagen, Madison, Wisc.). Cells were grown in M9 minimal media; consisting of 6 g/L $Na_2HPO_4.7H_2O$, 3 g/L KH_2PO_2, 0.5 g/L NaCl, 1 mM $MgSO_4$, 300 μM $CaCl_2$ supplemented with 0.5g/L $^{15}NH_4Cl$. Cells were induced at OD_{600} 0.7 with 1mM IPTG (Sigma-Aldrich, St. Louis, Miss.) for 3 hours at 37°C. After induction cells were pelleted by centrifugation (Avanti J26XP, Beckman Coulter, Brea, Cali.) and stored at -80°C .

Cell pellets were suspended in 50 mM Tris-HCl, pH7.4, 0.5 M NaCl containing protease inhibitors (EDTA free protease inhibitor cocktail, Roche, Basel, Switzerland) and heated to 90°C for 10 minutes in a water bath (VWB2, VWR, Radnor, Penn.). Resulting lysate was clarified by centrifugation at 20,000g for 30 minutes at 4°C and diluted into buffer A (50mM Tris-HCl, pH 7.4). Diluted lysate was loaded onto a 5 mL Hitrap Q column (Sigma-Aldrich, St. Louis, Miss.) pre-equilibrated with buffer A. Protein was eluted with a gradient of buffer B (50mM Tris-HCl, pH 7.4, 1 M NaCl). Fractions with a high absorbance at 280 nm were assayed by SDS-gel electrophoresis, pooled, concentrated and run on a Superdex S75 size exclusion column (Sigma-Aldrich, St. Louis, Miss.). Elution of αSyn occurred at a position equivalent to a 60 kDa folded protein, which is consistent with a disordered protein. Supporting this observation is the diffusion coefficient and chemical shifts observed by NMR, both of which are consistent with monomeric disordered protein. Subsequent purity was assayed by SDS-gel electrophoresis. Pure fractions were pooled, buffer exchanged and concentrated into 50 mM citric acid, 100 mM sodium phosphate, 2 mM sodium azide, pH 5 with Amicon concentrators (Millipore, Burlington, Mass.), and stored at -80°C for future use.

Source of GCase

GCase (VPRIV) was a gift from Shire Pharmaceuticals PLC (Dublin, Ireland). VPRIV is an enzyme replacement therapeutic for Gaucher's disease. VPRIV is produced from human cell lines supplemented with kifunensine resulting in high mannose glycans favourable for enzyme replacement therapy(53).

Lipid and detergent preparation

Single unilaminar vesicles (SUVs) and micelles were produced as previously outlined (44). It is important to have a preparation that does not precipitate and is kinetically stable under the solution conditions investigated. Stock solutions of DMPS, POPG, SDS and taurocholate were prepared in 50 mM citric acid, 100 mM sodium phosphate, 2 mM sodium azide (pH 5). DDM was mixed in with POPG and SDS to reduce the affinity of αSyn providing more signal intensity in the spectrum. Stock solutions were mixed at 50°C in a Thermomixer (ThermoFischer, Waltham, Mass.) for 4 hours, freeze thawed with a combination of a 50°C water bath (VWB2, VWR) and dry ice 5 times, before sonication for 5 minutes. Stock solutions were then immediately diluted to their working concentration. All lipid concentrations are stated where they were used in the manuscript, and all are above the critical concentration of the specified lipid/detergent.

$^{13}CH_3$ methyl labelling of GCase

It was necessary for this work to devise a labelling protocol for human cell line derived GCase. Labelling of arginine and lysine residues was accomplished by incubating with ^{13}C formaldehyde, using methods previously described(54). GCase was buffered in 50 mM citric acid, 100 mM sodium phosphate, 2 mM sodium azide (pH 5) or 50 mM citric acid, 100 mM sodium phosphate, 2 mM sodium azide (pH 7). Borane dimethylamine complex (Sigma-Aldrich, St. Louis, Miss.) was added to dilute (10 μM) GCase at 4°C to a final concentration of 20 μM. Immediately, ^{13}C formaldehyde (Sigma-Aldrich, St. Louis, Miss.) was added to a final concentration of 40 μM and the solution incubated on ice at 4°C for 2 hours. This was repeated once and incubated for a further two hours. Finally, Borane dimethylamine is added to a final concentration of 10μM and the reaction incubated overnight at 4°CC. The reaction was quenched by the addition of Trizma (pH 7) (Trizma, Sigma Aldrich, St. Louis, Miss.) to a final concentration of 100 mM. Reaction byproducts are then removed using Amicon concentrators (Millipore, Burlington, Mass.), washing with a buffer containing fresh 50 mM citric acid, 100 mM sodium phosphate, 2 mM sodium azide (pH 5) buffer.

LCMSMS and Methyl assignment

In order to assign the observed residues, LCMSMS experiments were performed. Peptides were re-suspended in 5% formic acid and 5% DMSO. They were separated on an Ultimate 3000 UHPLC system (ThermoFischer, Waltham, Mass.) and electrosprayed directly into an QExactive mass spectrometer (ThermoFischer, Waltham, Mass.) through an EASY-Spray nano-electrospray ion source (Thermofischer, Waltham, Mass.). The peptides were trapped on a C18 PepMap100 pre-column (300 μm i.d. x 5 mm, 100 , ThermoFisher, Waltham, Mass.) using solvent A (0.1% Formic Acid in water) at a pressure of 500 bar. The peptides were separated on an in- house packed analytical column (75 μm i.d. packed with ReproSil- Pur 120 C18-AQ, 1.9 μm, 120 , Dr. Maisch GmbH) using a linear gradient (length: 60 minutes, 7% to 28% solvent B (0.1% formic acid in acetonitrile), flow rate: 250 nL/min). The raw data was acquired on the mass spectrometer in a data-dependent mode (DDA). Full scan MS spectra were acquired in the Orbitrap (scan range 350-2000 m/z, resolution 70000, AGC target 3e6, maximum injection time 100 ms). After the MS scans, the 20 most intense peaks were selected for HCD fragmentation at 30% of normalised collision energy. HCD spectra were also acquired in the Orbitrap (resolution 17500, AGC target 5e4, maximum injection time 120 ms) with first fixed mass at 180 m/z.

NMR spectra acquired at pH 5 of GCase (VPRIV) pre-treated with formaldehyde at either pH 5 or pH7 under otherwise identical conditions yielded different spectra (Fig S5). In both cases, only one methyl addition was identified by LCMSMS to present under each condition as described in the text. This led to unambiguous assignment of R120, the only isolated, well dispersed peak structurally proximal to the active site E340 and E235 residues (55). K346, the other methyl identified by LCMSMS led to no obvious change in the NMR spectrum, suggesting its resonance overlays significantly in the centre of the spectrum.

GCase activity assays

GCase activity was performed in triplicate in 96-well clear flat bottom black polystyrene microplates (Product #3904, Corning) with 120 μM substrate (resorufin-β-D-glucopyranoside (Sigma-Aldrich, St. Louis, Miss.)) and 50 nM GCase buffered in 176 mM K_2HPO_4, 10 mM sodium taurocholate, 50 mM citrate, 0.01% tween 20, pH 5.9. The final well volume was 0.1ml. Fluorescence of hydrolysed substrate was measured on a Flurostar Omega (584/630 nm excitation and emission respectively) (BMG Labtech, Ortenberg, Germany) at 37°C (56).

Aggregation assays

Protein aggregation was observed via thioflavin-T (ThT) fluorescence in 96 microwell plates and a Fluostar Optima plate reader (BMG Labtech, Ortenberg, Germany). Microwell plates containing αSyn were aggregated either at 200 μM, 45°C or 100 μM, 30°C pH 5 in 50 mM citric acid, 100 mM sodium phosphate, 2 mM sodium azide pH 5. An *in-situ* ThT binding assay with 10 μM ThT and 440/490 nm excitation/emission filters monitored aggregation. ThT assays were repeated in triplicate yielding standard deviations for error measurements (Fig 1).

NMR experiments

NMR experiments were performed on a Varian 600 MHz spectrometer with a 5-mm z-axis gradient triple resonance room temperature probe at 30°C. Isotopically labeled ^{15}N αSyn and ^{13}C GCase were buffered in 50 mM citric acid, 100 mM sodium phosphate, 2 mM sodium azide (pH 5) and concentrated to 100 μM using Amicon concentrators (Millipore, Burlington, Mass.). 2D ^{15}N-^{1}H HSQC spectra were recorded with 128 scans per transient with acquisition times of 67.5 ms, over 100 complex points and a 1 s relaxation delay. 2D ^{13}C-^{1}H HMQC were recorded with 64 scans per transient and an acquisition time of 0.064 s, over 100 complex points and a 1.5 s relaxation delay.

Diffusion pulsed field gradient experiments were used to characterize diffusion behaviour. The translational diffusion of specific resonances was determined using ^{1}H pulsed field gradient NMR experiments for all mixtures of αSyn, GCase and lipids/detergents described in the paper. In such experiments, signal intensity is attenuated according to the strength of an applied gradient (expressed here with respect to the maximum applied gradient strength) in a manner defined by the translational diffusion coefficient. Increased signal attenuation reveals a larger diffusion coefficient. PFG experiments were carried out over 11 gradient strengths with 256 scans per transient and an acquisition time of 0.5 s. The maximum gradient strength was 60 G cm^{-1}. The gradient duration was 0.002 s with a 0.15 s delay between gradients. NMRPipe was used to analyse spectra (57) and Sparky was used to pick peaks and prepare figures. Peaks were assigned by comparison to previously published assignments of αSyn (58). As not all peaks were assigned due to overlap, we have in total a 60% assignment of resonances that are clearly isolated, whose coverage that uniformly spans the entire sequence. Peak intensity was calculated from peak heights obtained using Sparky. C-terminal and N-terminal intensities represent the mean and standard deviation of the 20 most C or N terminal residues.

Isotope (^{15}N) enriched αSyn fibrils were pooled and diluted in 50 mM citric acid, 100 mM sodium phosphate, 2 mM sodium azide (pH 5) to a final 100 μM concentration. Stock samples were then split into two equal working samples. Labelled ($^{13}CH_3$) GCase was added to a single sample to a final concentration of 100 μM. 2D ^{1}H-^{15}N HSQC and ^{1}H-^{13}C HMQC data were collected as described above.

Electron microscopy

Carbon coated grids (Electron Microscopy Sciences, La Sagne, Switzerland) were incubated with diluted microwell sample (10 μM) for 2 minutes and post stained with 2% aqueous uranyl acetate (10 s) and washed with water droplets. Grids were then imaged on a transmission electron microscope (FEI Tecnai 12) operated at 120kV using a digital CCD camera (Ultrascan US1000, Gatan).

Thermodynamic modelling

The reduction in signal intensity was recorded for the first and last 20 residues of αSyn, owing to their highly similar reduced relative intensities, together with GCase as a function of changes in concentration of the three components in the system, αSyn, GCase and lipids. The changes in signal intensity were concentration dependent and so we sought an equilibrium-binding model that accounted for all data. The total concentrations were varied of each such that we had 7 measurements of both GCase, N and C-terminal αSyn signal, providing 21 intensity datapoints for each of the anionic lipids and detergents DMPS, SDS/DDM and POPG/DDM. The specific concentrations used were such that this number of datapoints is more than sufficient to characterise the specific K_Ds.

There are two challenges to account for these observations. The first is to identify which species are forming, and the second is to account for how the formation of these species affects the NMR signal intensity. We sought to determine the model that gives the best fit to the data, subject to the restraint that improved fitting from more complex models is tested for statistical significance by applying an F-test and determining the probability that this improvement came by chance. A <5% probability level was taken as the condition for statistical significance.

The problem involves three species, lipid SUVs/micelles, αSyn and GCase. From the three components, there are 5 binary combinations that can be formed. Should we choose to distinguish independent sites for binding on the N and C termini, the formation of each of these can be characterized by the following association equilibrium constants and definitions:

$$\begin{aligned} [Ls-] &= K_{ln}\,[-s-]\,[L] \\ [-sL] &= K_{lc}\,[-s-]\,[L] \\ [GL] &= K_{lg}\,[G]\,[L] \\ [-sG] &= K_{gc}\,[-s-]\,[G] \\ [Gs-] &= K_{gn}\,[-s-]\,[G] \end{aligned} \tag{1}$$

Where the representation -S- for αSyn denotes either an empty N/C termini. Replacing one of the '–' symbols with either an L (lipid) or G (GCase) implies occupancy. There are 4 corresponding ternary complexes, which can be similarly defined in terms relevant equilibrium constants:

$$\begin{aligned} [LsG] &= K_{nlg}\,[Ls-]\,[G] \\ [GsL] &= K_{clg}\,[-sL]\,[G] \\ [GsG] &= K_{sgg}\,([-sG] + [Gs-])\,[G] \\ [LsL] &= K_{sll}\,([-sL] + [Ls-])\,[L] \end{aligned} \tag{2}$$

The equilibria are restrained by total numbers of molecules through the following three mass balancing equations:

$$\begin{aligned} S_{tot} &= [-s-] + [Ls-] + [-sL] + [Gs-] + [-sG] + [LsG] + [GsL] \\ G_{tot} &= [G] + [Gs-] + [-sG] + [GL] + [GsL] + [LsG] + 2\,[GsG] \\ L_{tot} &= [L] + [Ls-] + [-sL] + [GL] + [GsL] + [LsG] + 2\,[LsL] \end{aligned} \tag{3}$$

Where S_{tot}, G_{tot} and L_{tot} are the total concentrations of αSyn, GCase and lipids respectively. For known values of the total concentrations, and trial values of the relevant equilibrium constants, we can self-consistently solve these equations to obtain the corresponding mole fractions of the individual species. By optimising the equilibrium constants against experimental measures of mole fractions, we can obtain their most probable values.

To do this, it is necessary to obtain expressions for the observed signal intensity. There are a number of ways in which this can be formulated depending on the precise details of timescales of the interactions. The timescale together with the specific

structural changes that accompany the association will affect the signal intensities through chemical exchange. As described in the text, as we observe neither appreciable line broadening nor change in the chemical shift of resonances, we expect slow or slow-intermediate exchange. Moreover, no variation in the R^2 of the residues was observed with 180° pulse frequency in CPMG experiments, suggesting no species interconversion on the milli-second exchange.

If a species rigidly tumbles like either GCase or SUV/micelle, we would not expect it to contribute directly to the solution NMR spectra. Nevertheless, if part of αSyn retains some of its conformational flexibility when bound, we would expect it to contribute to the spectrum, although with a reduced signal intensity. To account for this type of interaction, and to first order to account for the effects of chemical exchange, the relaxation correction factors γ are introduced such that we can express the observed signal intensities as:

$$\begin{aligned}\left(\frac{I}{I_0}\right)_{\alpha Syn,N} &= \frac{[-s-] + [-sL]\,\gamma_1 + [-sG]\,\gamma_2}{S_{tot}} \\ \left(\frac{I}{I_0}\right)_{\alpha Syn,C} &= \frac{[-s-] + [Ls-]\,\gamma_3 + [Gs-]\,\gamma_4}{S_{tot}} \\ \left(\frac{I}{I_0}\right)_{GCase} &= \frac{[G] + [-sG]\,\gamma_5 + [Gs-]\,\gamma_6}{G_{tot}}\end{aligned} \tag{4}$$

The most complex model described by this picture is parametrized by 19 values (9 equilibrium constants including the ternary species and 10 attenuation constants). This model was found to provide the best fit to the data. But as we have 21 individual signal intensity measurements, to apply this model carries a strong risk of over-fitting. We tested a number of models both including and excluding ternary complexes, and with varying numbers of species included that are proposed to be NMR observable (non zero γ factors).

Following the principles of sensible fitting, we sought to determine the minimally complex model where the reduction in χ^2 to more complex models is determined to be statistically insignificant by application of an F-test. The χ^2 was defined as:

$$\chi^2 = \sum_{concentration} \sum_{\alpha Syn,N,\alpha Syn,C,GCase} \left(\left(\frac{I}{I_0}\right)_{calculated} - \left(\frac{I}{I_0}\right)_{measured}\right)^2 \tag{5}$$

Such testing revealed that no significant improvement was obtained if we incorporate 1) lipids binding the C-terminus of αSyn, 2) GCase binding the N-terminus of GCase, nor 3) any of the ternary complexes. Moreover, there was no statistical benefit to including observation of GCase signal when it is bound to lipids. This results in the following simplified model that we conclude gives the best statistical fit to the data, with three equilibrium constants:

$$\begin{aligned}[Ls-] &= K_{ln}\,[-s-]\,[L] \\ [GL] &= K_{lg}\,[L]\,[G] \\ [-sG] &= K_{gc}\,[-s-]\,[G]\end{aligned} \tag{6}$$

And three attenuation exchange factors whose origin comes from chemical exchange (γ):

$$\begin{aligned}\left(\frac{I}{I_0}\right)_{\alpha Syn,N} &= \frac{[-s-] + [-sG]}{S_{tot}} \\ \left(\frac{I}{I_0}\right)_{\alpha Syn,C} &= \frac{[-s-] + [Ls-]\,\gamma_{\alpha Syn(C)}}{S_{tot}} \\ \left(\frac{I}{I_0}\right)_{GCase} &= \frac{[G] + [-sG]\,\gamma_{GCase}}{G_{tot}}\end{aligned} \tag{7}$$

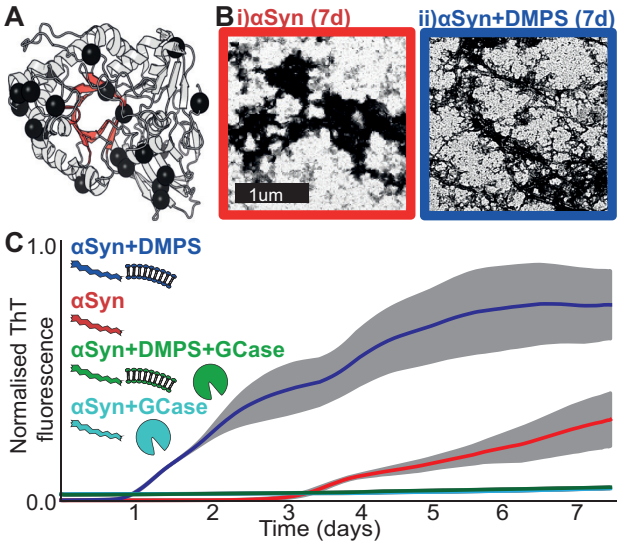

Figure 1: **A)** A structure of GCase (PDB 1OGS) showing mutation sites linked to PD (60) (black), together with the active site (red). **B)** Negatively stained electron micrographs reveal aggregation of αSyn and αSyn+DMPS samples at pH 5 after 7 days. Though they stain with ThT and the aggregates have a fibrillar aspect, discrete fibrils were not observed. **C)** αSyn aggregation kinetics were monitored by a thioflavin-T (ThT) assay at pH 5 with DMPS (blue), GCase (cyan) and both (green). Aggregation of αSyn (red) is promoted by DMPS (blue) and inhibited by GCase both with and without DMPS (cyan/green). The grey band shows the standard deviation of 3 independent measurements.

This model (Fig S6, model 3, S7) is not significantly improved over a model where we set $\gamma 3$ to 1, which amounts to the N-terminus of αSyn contributing to the observed signal intensity equally to free αSyn. Overall this model (Fig S6, model 4) is parametrized by 5 constants and predicts the existence of 3 binary complexes in addition to the 3 free species. This model gives an excellent description of all signal intensities recorded over the wide range of combinations of concentrations tested. Incorporating additional parameters did not result in a statistically significant improvement in the fitting. The formulation of the signal intensities successfully account for the observed increase in diffusion coefficients (Fig S4) as it predicts bound species contribute the spectrum albeit with reduced signal intensity when compared to the free species.

The code to perform this analysis was written in python, where it was determined that a stimulated annealing approach was necessary to find the global optimum. Uncertainties in fitting parameters were derived from a Monte-Carlo method, with between 20% and 30% uncertainty in each parameter. The uncertainty is relatively high. The trends in these parameters however span orders of magnitude (Fig 6B) and so we obtain meaningful mechanistic insight with this approach. The high uncertainties also imply that incorporation of additional information into the model, for example a more detailed description of chemical exchange parametrized with additional data could further refine the model. The optimal model does not include ternary complexes. We note that this does not mean ternary complexes cannot form, just that we see no statistically significant reason in the data to justify their inclusion to quantitatively explain the data, suggesting if they are formed they are highly unstable. The formation of ternary complexes has been previously inferred from fluorescence changes (59) though this finding is not supported by our data on the mixtures analysed here.

RESULTS

GCase inhibits αSyn amyloidogenesis under lysosomal conditions

To mimic the amyloidogenesis of αSyn in the lysosome, αSyn aggregation was monitored using the amyloid specific dye thioflavin-T (ThT) at pH 5 in the presence and absence of both GCase and assemblies of anionic lipids (Figure 1) (44, 50). The aggregation of αSyn at pH 5 was markedly faster in the presence of DMPS, reducing the lag time from 3 days (red), to 1 (blue) (Figure 1B/C). Although the aggregates bound ThT and possessed fibrillar morphological aspects, discrete fibrils were not observed in electron micrographs (Figure 1B). Remarkably, adding GCase effectively prevented aggregation both in

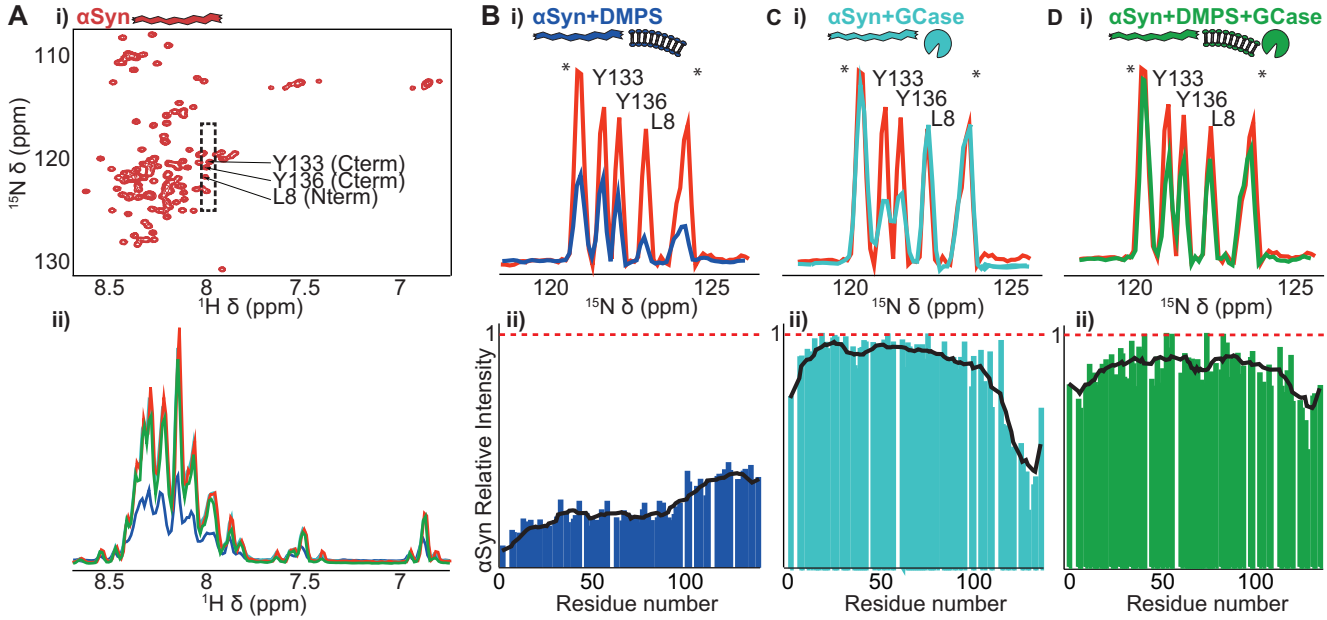

Figure 2: GCase rescues αSyn from lipid binding under lysosomal conditions. **A)** i) A lack of αSyn signal dispersion in a 2D ^{1}H-^{15}N HSQC spectrum confirms its intrinsically disordered character. ii) Incubating αSyn (red) with the anionic lipid DMPS (blue) attenuates the intensity of all signals due to formation of high molecular weight complexes, whereas the addition of GCase (green) recovers it. In **B**, **C**, and **D**, the (i) same 2D ^{1}H-^{15}N HSQC region (see box in Ai) and (ii) corresponding αSyn signal intensities are shown in the absence or presence of DMPS or GCase, respectively, relative to the signal intensity of free αSyn. Addition of GCase significantly increases the amount of free αSyn present in solution.

the presence (cyan) and absence (green) of DMPS, demonstrating that it is a potent inhibitor of αSyn amyloidogenesis under lysosomal conditions.

GCase and anionic lipids compete for opposite termini of monomeric αSyn

In order to understand the molecular basis of this interaction, we recorded fingerprint ^{15}N-^{1}H HSQC NMR spectra in absence and presence of DMPS, POPG, SDS, DDM, and tween under otherwise identical lysosomal conditions. In a ^{1}H-^{15}N HSQC spectrum, one resonance is observed for each distinct HN environment in the molecule. ^{1}H NMR resonances fell predominantly in the region 8-8.5 ppm, confirming the expected disordered character of αSyn (Fig 2A).

In the presence of the anionic taurochlorate, DMPS and 1:1 mixtures of DDM with SDS and POPG (Fig S1) a residue specific reduction in signal intensity was observed, with no significant change in either resonance frequencies or observed linewidths (fig 2Aii, S2, S3). In line with previous observations, N-terminal αSyn residues showed a greater decrease in signal intensity than those in the C-terminus (Fig 2B, S2). Moreover, a higher lipid ratio decreased the N-terminal NMR signal intensities further (Fig S2). By contrast, micelles formed from the non-ionic detergents DDM and tween resulted in no change in signal intensity (Fig S3). In the case of the anionic lipids, the observed diffusion coefficients of αSyn were significantly reduced (Fig S4). Together, the loss in signal intensity can be explained by the formation of αSyn lipid complexes, where any structured portion of the molecule tumbles too slowly to be observed directly by solution state NMR.

Next we determined the effect of GCase on αSyn in a 1:1 mixture of both components. Contrasting with lipid binding, a signal intensity reduction was observed localized to the C-terminus of αSyn (Fig 2C). Incubation of αSyn in the presence of lipids and GCase (figure 2D) resulted in a recovery of signal intensity in both the N- and C-termini. Furthermore, NMR diffusion coefficients of αSyn returned to values similar to those measured for the isolated form (Fig S4). These results indicate that GCase substantially rescues αSyn from its lipid-bound amyloidogenic state.

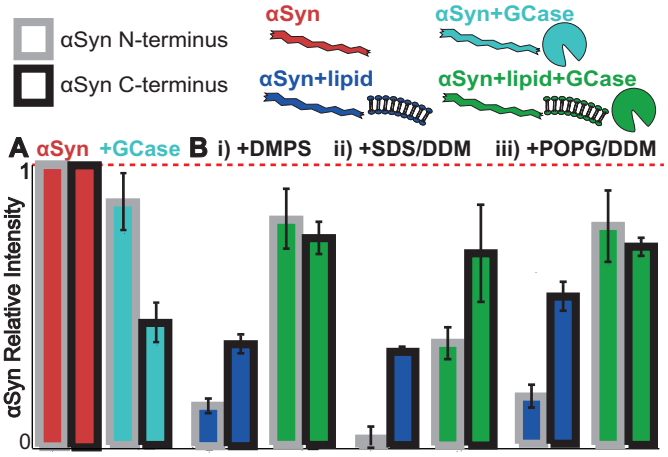

Figure 3: Integrated relative signal intensities and between residue standard deviations of the 20 most N- (grey) and C- (black) terminal αSyn residues in the presence of GCase (cyan), anionic lipid SUVs/micelles formed from DMPS,SDS/DDM, or POPG/DDM (blue) and their combination (green). In each case there is substantial recovery in the observed signal intensity by adding GCase (green).

To allow for a quantitative comparison of the effects at the N- and C- termini of αSyn, the signal intensities of the first and last 20 residues were integrated for each of the mixtures of αSyn with GCase and lipid SUVs/micelles (Fig 3,S2C,S3F/G). Although the magnitudes of the interaction of αSyn with different lipids vary, GCase was always found to rescue the signal intensity of αSyn (Fig 3).

GCase destabilises mature αSyn amyloid fibrils

We sought to examine the effect of GCase on pre-formed amyloid fibrils. At elevated temperatures and concentrations (200 μM, 45°C) ^{15}N labelled αSyn showed increased ThT fluorescence (Fig 4A), and discrete amyloid fibrils were observed by EM (Fig 4B) (44). A ^{1}H-^{15}N HSQC NMR spectrum of these samples at pH 5 revealed a small population of flexible C-terminal residues observable by NMR, a finding in agreement with proteolysis and solid state NMR studies (35, 61, 62). Most remarkably, addition of GCase to these samples recovered signal from N-terminal residues (Fig 4C), indicating a destabilization of the amyloid form and partial rescue of monomeric αSyn by GCase.

GCase interacts with αSyn near its active site

Post-translational modifications are vital for active and stable GCase (30, 63, 64). While protein with these modifications can be prepared from human cell lines, introducing the necessary isotopes for NMR analysis during expression is prohibitively expensive. Moreover, the high molecular weight of GCase (60 KDa) would significantly broaden the width of observed NMR resonances in a protonated sample. To overcome this, we introduced ^{13}C ^{1}H$_3$ methyl groups to specific locations on the protein surface. The large number of equivalent protons and rapid internal dynamics result in to sharp resonances in NMR spectra, making such probes highly desirable for large molecular weight proteins.

To incorporate ^{13}C^{1}H$_3$ methyl groups into human cell derived GCase containing human post translational modifications, we employed chemical modification. Amine methylation is a routine strategy in crystallography and although it leads to covalent modification, protein structure and interactions are not generally perturbed (49, 54, 65–69). To maximize coverage of the protein surface, we targeted lysine and arginine residues using ^{13}C labeled formaldehyde (67, 70) rather than targeting the smaller number of cysteine residues (71).

GCase (Shire PLC) was produced from human cell lines and then incubated with ^{13}C formaldehyde to produce lys^{13}C^{1}H$_3$

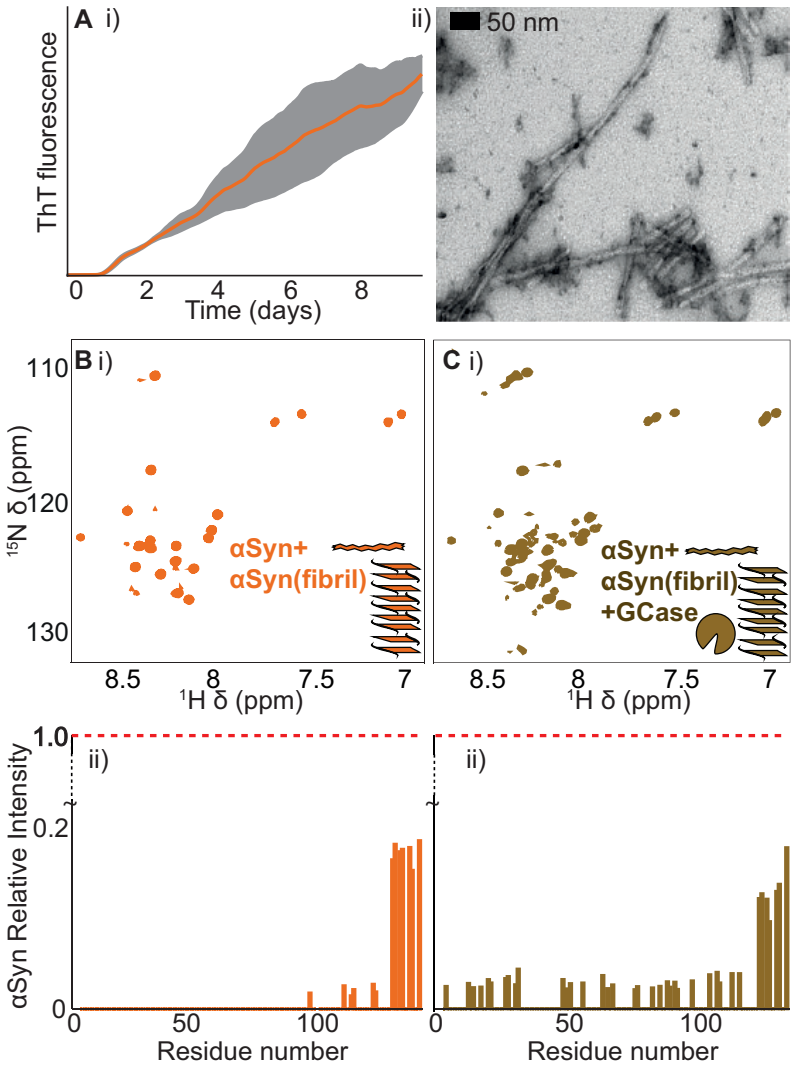

Figure 4: **A)** i) The αSyn aggregation kinetics were monitored by a thioflavin-T fluorescence assay at elevated temperature and concentration (45^{o}C, 200 μM) at pH 5. ii) These conditions result in discrete amyloid fibrils, as observed by EM. **B/C)** Amyloid fibrils were purified by ultra centrifugation, and its ^{1}H-^{15}N HSQC NMR spectrum was taken (Bi, orange). GCase was then added and the spectrum was obtained (Ci, brown). All spectra were acquired under lysosomal conditions (pH 5). ii) The relative intensity of the oserved resonances as a function of residue position in the αSyn sequence. Incubation with GCase results in a significant release of free αSyn.

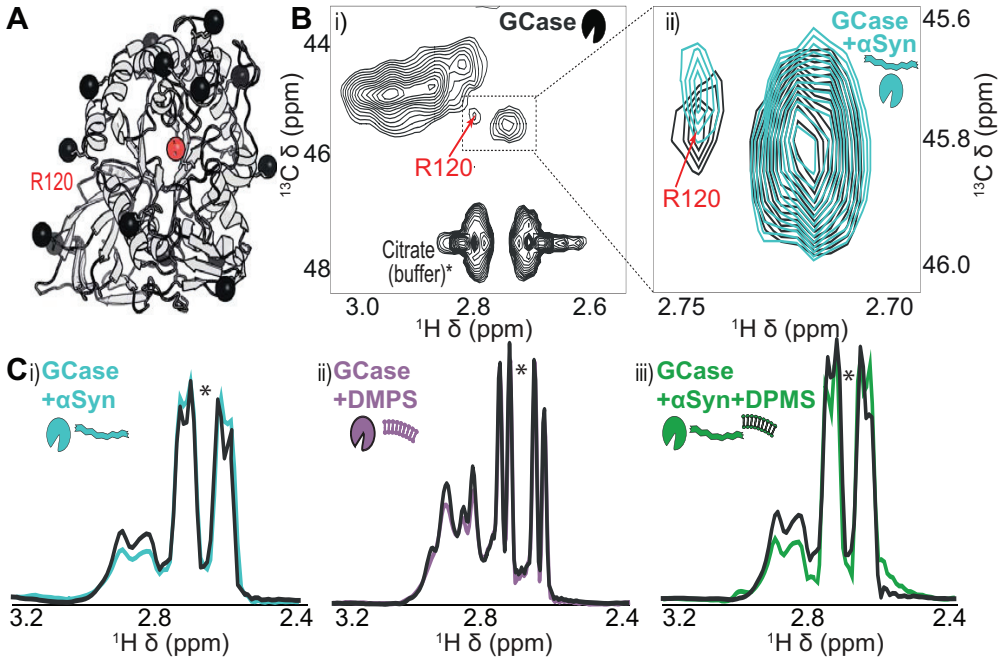

Figure 5: **A)** Lysine and arginine residues on the surface of GCase (PDB 1OGS) were modified by incubation with ^{13}C labelled formaldehyde (black spheres, see Fig S5). **B)** i) 2D ^{1}H-^{13}C HMQC NMR spectrum of the labelled residues. Natural abundance of ^{13}C citrate results in sharp resonances in the indicated positions (*). While the majority of resonances overlap, one distinct peak from R120 could be distinguished and unambiguously assigned using LCMSMS (Fig S5). ii) After incubation with αSyn, the locations of all the resonances were largely unchanged. Only the resonance corresponding to R120 was found to move, suggesting a direct interaction between this site and αSyn. **C)** ^{1}H projections of 2D spectra after arginine methylation (black) and mixtures with αSyn and anionic lipids (cyan/purple/green). As GCase samples were prepared independently, small fluctuations in spectra between samples were observed (black i,ii,iii). The small differences in signal intensity from the citrate in projection are due to truncation artefacts in the spectra, and do not reflect changes in citrate concentration. The uniform loss of signal intensity from resonances originating from GCase after incubation with αSyn, DMPS or a mixture of both indicates the formation of high molecular weight species that are not directly observed.

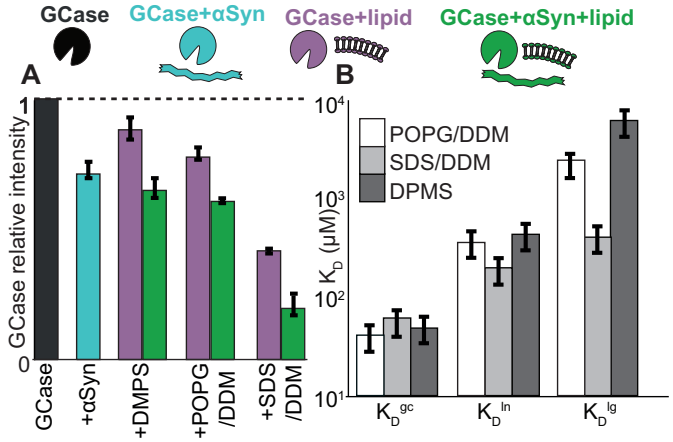

Figure 6: **A)** Summary of the changes in resonance intensity of $^{13}C^1H_3$ labelled GCase on incubation with αSyn (cyan), lipids DMPS, POPG/DDM, SDS/DDM (purple), and both αSyn and lipid (green). **B)** Quantitative K_D values for the three processes from fitting the combined αSyn, GCase and lipid binding data to optimal model (Fig S6,S7). The dissociation constant for GCase/αSyn complex formation was independent of lipid choice. The specific K_Ds for both αSyn and GCase lipid binding are highly dependent on the choice of lipid, and are highly correlated. The strongest binding was observed with SDS/DDM, and the weakest with DMPS. K_D^{gc} describes the interaction between the C-terminus of αSyn and GCase, K_D^{ln} describes the interaction between the N-terminus of αSyn and lipids, and K_D^{lg} describes the interaction between GCase and lipids.

and arg$^{13}C^1H_3$ enriched GCase (methods). The successful modification of specific lys and arg residues was confirmed by liquid chromatography tandem mass spectrometry (LCMSMS) (Fig S5) with no significant change in activity (Fig S5D). Most resonances in the ^{1}H-^{13}C HMQC spectra were heavily overlapped due to a combination of low chemical shift dispersion, a large number of labels and the intrinsically slow tumbling of the 60 kDa protein leading to broadened resonances (Fig 5B). By analysis of additional 2D ^{1}H-^{13}C HMQC spectra and comparison to LCMSMS data under different methylation conditions, however, one resonance could be unambiguously assigned to the active side residue R120 (72) (Fig S5).

The $^{13}C^1H_3$ methyl groups were used to monitor the effects of both lipids and αSyn on GCase (Fig 5C,6A). The addition of either αSyn or DMPS resulted in decreased GCase signal intensity. Most notably, a modest yet significant change in the chemical shift of the peak arising from R120 was observed on mixing with αSyn, whereas the resonance frequencies of the remaining residues were largely unchanged. This suggests that the interaction site is in the vicinity of this location. As R120 is close to the active site, this observation is consistent with αSyn reducing the activity of GCase (20, 59) and with FRET data (59).

GCase prevents αSyn aggregation through a competitive equilibrium

Our data allows us to follow the interactions between αSyn, lipids and GCase from the perspective of αSyn and GCase. The loss of signal intensities in both αSyn and GCase were both reversible, and dependent on the concentrations of the three species (Fig 2,3,4,6,S2,S3) revealing that these two species on the timescale of the NMR experiments are in competition with lipids. We sought to determine whether a simple equilibrium model could explain our combined datasets. To do these, we needed to analyse the possible origin of intensity losses in our NMR spectra. Having explored a large range of different concentrations of the three reagents, coupled to the large number of probes reporting on various structural regions of both αSyn and GCase, our datasets are well suited to providing significant insight into the mechanism by which the three interact.

As their slow tumbling prohibits a direct observation of SUVs and GCase in ^{1}H NMR spectra, we would also not expect to observe regions of αSyn directly bound to either lipids or GCase. Consequently, complex formation is registered in the form of a loss of NMR signal intensity. If only one terminus of αSyn bound SUV or GCase, the other terminus would remain flexible and detectable by NMR. This allows not only for a differential analysis of both termini but also a quantification of attenuated NMR signal intensities.

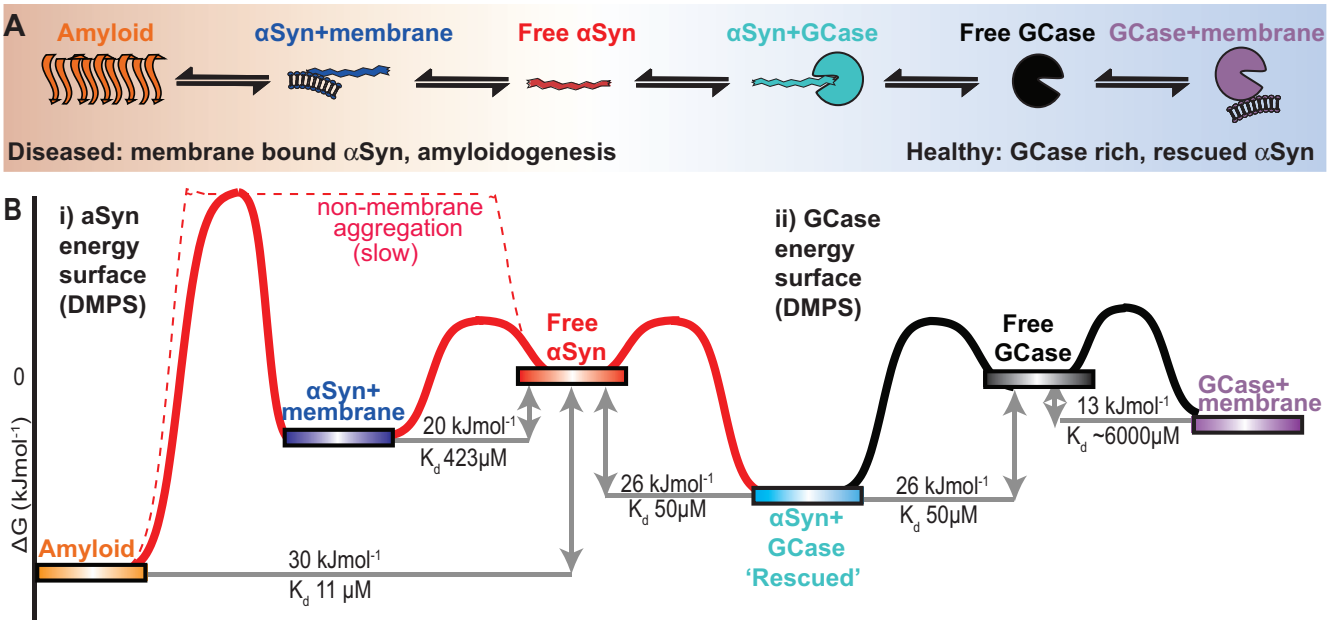

Figure 7: A quantitative equilibrium competition model between αSyn, GCase and lipid well explains all of our data. αSyn aggregation is accelerated by the presence of anionic lipids (Fig 1). GCase binding greatly inhibits this process, inhibiting αSyn amyloidogenesis (Fig 1). **B)** A schematic free energy surface for DMPS displays how all complexes are related. The presence of αSyn- GCase complexes effectively rescues αSyn by preventing their build up on the surface of membranes. The energy landscape is shown from the perspective of αSyn (i) and from GCase (ii). All binding reactions came to equilibrium at maximum on the timescale of a few minutes, whereas αSyn aggregation occurs on a timescale of days under these conditions. The uncertainties of the specific free energies can be propagated from the values in figure S7A.

As we did not observe any line broadening, chemical shift perturbations(32, 33, 73), or variations in CPMG-derived transverse relaxation rates (data not shown) of αSyn residues, our results suggest that chemical exchange is in slow or slow-intermediate limits (32, 73, 74). We account for these effects in the NMR spectra by allowing regions of αSyn that are expected to retain significant flexibility to contribute to the NMR spectrum in a manner that is proportional to the concentration of complex formed, thought reduced from that of the free state (methods). This exchange regime is also consistent with the reduced diffusion coefficients observed upon binding (Fig S4).

Subsequently, we tested a wide range of possible binding models (Fig S6) and used F-tests to identify the simplest model explaining all of the data, while avoiding over-fitting (methods). The simplest model tested considers only binary complexes and does not distinguish between binding to the N- and the C-termini of αSyn, whereas the most complex model included all possible ternary complexes (Fig S6). The optimal model explains all of our data quantitatively (Fig. S7), considers all interactions with DMPS, POPG/DDM, and SDS/DDM, is consistent with the decreased diffusion coefficients (Fig. S4). It allows for both GCase and the N-terminus of αSyn to bind lipids, and the C-terminus of αSyn to bind GCase. It is parametrized by three dissociation constants for the formation of complexes between GCase and lipids (K_D^{lg}), the C-terminus of αSyn and GCase (K_D^{gc}) and the N-terminus of αSyn and lipids (K_D^{ln}) (Fig S6,S7). It also takes attenuated NMR signal intensities of an αSyn terminus into account when the opposite terminus is involved in complex formation (methods).

Overall, the model reveals simple equilibrium binding where the N- and C-termini of αSyn are in competition with lipids and GCase, respectively (Fig 6B,S7). The K_D^{gc} for the GCase/αSyn(C) interaction was ca. 60 μM for all lipids tested, whereas the K_D^{ln} for the αSyn(N)/lipid interaction followed the degree of charge on the lipid head group in the sequence DMPS, POPG/DDM, SDS/DDM. It is interesting to note that the lipids that bound GCase more tightly also had a higher affinity for αSyn suggesting that αSyn and GCase compete for similar binding sites on the surface of lipids.

All of the data can be quantitatively summarized on a free energy surface (Fig 7). Free αSyn (red) will form amyloids (orange) if left for sufficient time. This process is greatly accelerated by anionic lipids (blue, Fig 1). GCase effectively competes with lipids for binding of αSyn (cyan). By reducing the population of lipid bound complexes GCase prevents the build-up of amyloidogenic

precursors to inhibit amyloid formation. If left for long enough, stable amyloid formation is expected to become inevitable (75). Yet the formation of rapid and relatively weak contacts between GCase and αSyn greatly curtails amyloidogenesis.

DISCUSSION

Here, we demonstrate that GCase directly inhibits amyloidogenesis of αSyn both in the presence and absence of anionic lipids under lysosomal solution conditions (Fig 1). Quantitative analysis of the changes in both GCase and αSyn reveals a molecular 'tug of war' mechanism in which GCase and anionic membrane mimics are in competition for the C- and N-termini of αSyn respectively (Fig 2). The strongest interaction identified here between GCase and the C-terminus of αSyn inhibits amyloidogenesis, revealing a protective role for GCase in PD pathology. Though not explicitly characterised here, complexes between αSyn and GCase clearly inhibit the formation of αSyn aggregation nuclei both on and off lipids (Fig 1). These results demonstrate that GCase can function as a molecular chaperone, reversibly binding αSyn and both inhibiting the formation and reducing the stability of amyloid formed from αSyn.

Central to the determination of this mechanism was the need to study human cell derived GCase complete with relevant post-translational modifications. The methylation methodology we employ is generally applicable for studies of biologically relevant proteins without the need to be prepared in lower organisms.

In a healthy lysosome, a GCase rich lysosome is able to degrade both monomeric αSyn and αSyn oligomers (6, 15, 17). In PD, depletion of GCase in the lysosome is associated with the build-up of amyloid and enhanced susceptibility to Parksinson's disease (5, 8, 11, 14, 15, 17, 20, 21, 76, 77). αSyn amyloidogenesis in the lysosome is enhanced by both GCase depletion, and the presence of anionic lipids (4, 5, 14, 15, 17, 20, 27). GCase depletion also enhances the transfer of αSyn oligomers between cells by the lysosomal system (20, 25, 26). The presence of anionic lipids and mutations that deplete the lysosomal GCase concentration are both significant risk factors in PD. Our model explains these observations, predicting a shift in equilibrium favouring increased lipid-induced amyloid formation in the case of GCase depletion under lysosomal conditions. Furthermore, GCase's destabilising role on amyloid fibrils explains why the depletion of GCase results in an enhanced transfer of αSyn oligomers between lysosomes of adjacent cells (20, 25, 26).

Taken together, our quantitative analysis explains the protective effect of GCase on PD models and why its genetic and sporadic depletion results in an increased risk of PD (13, 78). We demonstrate that wild-type GCase can function as a molecular chaperone, inhibiting αSyn amyloid formation under lysosomal conditions. These results provide a molecular framework to interpret the potential therapeutic benefits of GCase in Parkinson's disease.

CONCLUSION

The lipid-accelerated deposition of αSyn into amyloid rich Lewy bodies is a key hallmark of Parkinson's disease. Recently, lysosomal enzyme glucocerebrosidase has been implicated in sporadic and non-sporadic Parkinson's disease. Here, we have shown by solution state NMR the protective role of human-cell derived GCase in inhibiting αSyn amyloid formation and disrupting pre-formed amyloid fibrils under lysosomal conditions. We have further localised interaction sites using human cell derived GCase. And proposed a "tug of war" mechanism where GCase and lipids compete for different termini of αSyn, explaining the relationship between GD and PD.

AUTHOR CONTRIBUTIONS

MB led the design and execution of the research with AB, AB led the statistical modelling of the NMR data with MB. HM provided expertise in electron microscopy and RG aided with molecular biology techniques.

ACKNOWLEDGEMENTS

AJB thanks the BBSRC for a David Phillip's Fellowship. MB thanks the BBSRC for Doctoral Training Partnership funding. The authors thank T.R. Alderson for the αSyn plasmid and Shire PLC for GCase (VPRIV) samples. The Division of Structural Biology is a part of the Wellcome Trust Centre for Human Genetics, Wellcome Trust Core Grant Number 090532/Z/09/Z.

REFERENCES

1. Trojanowski, J. Q., and V. M. Y. Lee, 2002. Parkinson's disease and related synucleinopathies are a new class of nervous system amyloidoses. *Neurotoxicology* 23:457–60. http://www.ncbi.nlm.nih.gov/pubmed/12428717.

2. Beavan, M. S., and A. H. V. Schapira, 2013. Glucocerebrosidase mutations and the pathogenesis of Parkinson disease. *Annals of medicine* 45:511–21. http://www.ncbi.nlm.nih.gov/pubmed/24219755.

3. Alcalay, R. N., O. A. Levy, C. C. Waters, S. Fahn, B. Ford, S.-H. Kuo, P. Mazzoni, M. W. Pauciulo, W. C. Nichols, Z. Gan-Or, G. A. Rouleau, W. K. Chung, P. Wolf, P. Oliva, J. Keutzer, K. Marder, and X. Zhang, 2015. Glucocerebrosidase activity in Parkinson's disease with and without GBA mutations. *Brain : a journal of neurology* 138:2648–58. http://brain.oxfordjournals.org/content/138/9/2648.

4. Chiasserini, D., S. Paciotti, P. Eusebi, E. Persichetti, A. Tasegian, M. Kurzawa-Akanbi, P. F. Chinnery, C. M. Morris, P. Calabresi, L. Parnetti, and T. Beccari, 2015. Selective loss of glucocerebrosidase activity in sporadic Parkinson's disease and dementia with Lewy bodies. *Molecular neurodegeneration* 10:15. http://www.molecularneurodegeneration.com/content/10/1/15.

5. Murphy, K. E., A. M. Gysbers, S. K. Abbott, N. Tayebi, W. S. Kim, E. Sidransky, A. Cooper, B. Garner, and G. M. Halliday, 2014. Reduced glucocerebrosidase is associated with increased α-synuclein in sporadic Parkinson's disease. *Brain : a journal of neurology* 137:834–48. http://brain.oxfordjournals.org/content/137/3/834.longhttp://brain.oxfordjournals.org/content/137/3/834.

6. Goker-Alpan, O., B. K. Stubblefield, B. I. Giasson, and E. Sidransky, 2010. Glucocerebrosidase is present in α-synuclein inclusions in Lewy body disorders. *Acta neuropathologica* 120:641–9. http://www.pubmedcentral.nih.gov/articlerender.fcgi?artid=3352317{&}tool=pmcentrez{&}rendertype=abstract.

7. Wong, K., E. Sidransky, A. Verma, T. Mixon, G. D. Sandberg, L. K. Wakefield, A. Morrison, A. Lwin, C. Colegial, J. M. Allman, and R. Schiffmann, 2004. Neuropathology provides clues to the pathophysiology of Gaucher disease. *Molecular genetics and metabolism* 82:192–207. http://www.ncbi.nlm.nih.gov/pubmed/15234332.

8. Bultron, G., K. Kacena, D. Pearson, M. Boxer, R. Yang, S. Sathe, G. Pastores, and P. K. Mistry, 2010. The risk of Parkinson's disease in type 1 Gaucher disease. *Journal of inherited metabolic disease* 33:167–73. http://www.pubmedcentral.nih.gov/articlerender.fcgi?artid=2887303{&}tool=pmcentrez{&}rendertype=abstract.

9. McNeill, A., R. Duran, D. A. Hughes, A. Mehta, and A. H. V. Schapira, 2012. A clinical and family history study of Parkinson's disease in heterozygous glucocerebrosidase mutation carriers. *Journal of neurology, neurosurgery, and psychiatry* 83:853–4. http://www.pubmedcentral.nih.gov/articlerender.fcgi?artid=3927562{&}tool=pmcentrez{&}rendertype=abstract.

10. Rocha, E. M., G. A. Smith, E. Park, H. Cao, E. Brown, M. A. Hayes, J. Beagan, J. R. McLean, S. C. Izen, E. Perez-Torres, P. J. Hallett, and O. Isacson, 2015. Glucocerebrosidase gene therapy prevents α-synucleinopathy of midbrain dopamine neurons. *Neurobiology of disease* 82:495–503. http://www.sciencedirect.com/science/article/pii/S0969996115300504.

11. Liu, G., M. Chen, N. Mi, W. Yang, X. Li, P. Wang, N. Yin, Y. Li, F. Yue, P. Chan, and S. Yu, 2015. Increased oligomerization and phosphorylation of α-synuclein are associated with decreased activity of glucocerebrosidase and protein phosphatase 2A in aging monkey brains. *Neurobiology of aging* 36:2649–59. http://www.sciencedirect.com/science/article/pii/S0197458015003152.

12. Sardi, S. P., J. Clarke, C. Kinnecom, T. J. Tamsett, L. Li, L. M. Stanek, M. a. Passini, G. a. Grabowski, M. G. Schlossmacher, R. L. Sidman, S. H. Cheng, and L. S. Shihabuddin, 2011. CNS expression of glucocerebrosidase corrects alpha-synuclein pathology and memory in a mouse model of Gaucher-related synucleinopathy. *Proceedings of the National Academy of Sciences of the United States of America* 108:12101–12106.

13. Sardi, S. P., J. Clarke, C. Viel, M. Chan, T. J. Tamsett, C. M. Treleaven, J. Bu, L. Sweet, M. A. Passini, J. C. Dodge, W. H. Yu, R. L. Sidman, S. H. Cheng, and L. S. Shihabuddin, 2013. Augmenting CNS glucocerebrosidase activity as a therapeutic strategy for Parkinsonism and other Gaucher-related synucleinopathies. *Proceedings of the National Academy of Sciences of the United States of America* 110:3537–3542. http://www.ncbi.nlm.nih.gov/pubmed/23297226.

14. Lee, H.-J., F. Khoshaghideh, S. Patel, and S.-J. Lee, 2004. Clearance of alpha-synuclein oligomeric intermediates via the lysosomal degradation pathway. *The Journal of neuroscience : the official journal of the Society for Neuroscience* 24:1888–1896.

15. Cuervo, A. M., L. Stefanis, R. Fredenburg, P. T. Lansbury, and D. Sulzer, 2004. Impaired degradation of mutant alpha-synuclein by chaperone-mediated autophagy. *Science (New York, N.Y.)* 305:1292–1295.

16. Webb, J. L., B. Ravikumar, J. Atkins, J. N. Skepper, and D. C. Rubinsztein, 2003. α-synuclein Is Degraded by Both Autophagy and the Proteasome. *Journal of Biological Chemistry* 278:25009–25013.

17. Mak, S. K., A. L. McCormack, A. B. Manning-Bog, A. M. Cuervo, and D. a. Di Monte, 2010. Lysosomal degradation of α-synuclein in vivo. *Journal of Biological Chemistry* 285:13621–13629.

18. Bendikov-Bar, I., I. Ron, M. Filocamo, and M. Horowitz, 2011. Characterization of the ERAD process of the L444P mutant glucocerebrosidase variant. *Blood cells, molecules & diseases* 46:4–10. http://www.ncbi.nlm.nih.gov/pubmed/21106416.

19. Ron, I., and M. Horowitz, 2005. ER retention and degradation as the molecular basis underlying Gaucher disease heterogeneity. *Human Molecular Genetics* 14:2387–2398.

20. Mazzulli, J. R., Y.-H. Xu, Y. Sun, A. L. Knight, P. J. McLean, G. A. Caldwell, E. Sidransky, G. A. Grabowski, and D. Krainc, 2011. Gaucher Disease Glucocerebrosidase and α-Synuclein Form a Bidirectional Pathogenic Loop in Synucleinopathies. *Cell* 146:37–52. http://www.cell.com/abstract/S0092-8674(11)00601-5http://www.sciencedirect.com/science?{_}ob=GatewayURL{&}{_}origin=CELLPRESS{&}{_}urlversion=4{&}{_}method=citationSearch{&}{_}version=1{&}{_}src=FPDF{&}{_}piikey=S0092867411006015{&}md5=61618140179d8b2270489c6f49f26d50.

21. Gegg, M. E., D. Burke, S. J. R. Heales, J. M. Cooper, J. Hardy, N. W. Wood, and A. H. V. Schapira, 2012. Glucocerebrosidase deficiency in substantia nigra of parkinson disease brains. *Annals of neurology* 72:455–463. http://www.ncbi.nlm.nih.gov/pubmed/23034917.

22. Winder-Rhodes, S. E., J. R. Evans, M. Ban, S. L. Mason, C. H. Williams-Gray, T. Foltynie, R. Duran, N. E. Mencacci, S. J. Sawcer, and R. A. Barker, 2013. Glucocerebrosidase mutations influence the natural history of Parkinson's disease in a community-based incident cohort. *Brain* 136:392–399. http://brain.oxfordjournals.org/content/136/2/392http://brain.oxfordjournals.org/content/136/2/392.full.pdfhttp://www.ncbi.nlm.nih.gov/pubmed/23413260http://brain.oxfordjournals.org/content/136/2/392.long.

23. Bae, E.-J., N. Y. Yang, C. Lee, H.-J. Lee, S. Kim, S. P. Sardi, and S.-J. Lee, 2015. Loss of glucocerebrosidase 1 activity causes lysosomal dysfunction and α-synuclein aggregation. *Experimental & molecular medicine* 47:e153. http://www.ncbi.nlm.nih.gov/pubmed/25813221.

24. Nichols, W. C., N. Pankratz, D. K. Marek, M. W. Pauciulo, V. E. Elsaesser, C. A. Halter, A. Rudolph, J. Wojcieszek, R. F. Pfeiffer, and T. Foroud, 2009. Mutations in GBA are associated with familial Parkinson disease susceptibility and age at onset. *Neurology* 72:310–316. http://www.ncbi.nlm.nih.gov/pmc/articles/PMC2677501/http://www.ncbi.nlm.nih.gov/pmc/articles/PMC2677501/pdf/znl00409000310.pdf.

25. Bae, E.-J., N.-Y. Yang, M. Song, C. S. Lee, J. S. Lee, B. C. Jung, H.-J. Lee, S. Kim, E. Masliah, S. P. Sardi, and S.-J. Lee, 2014. Glucocerebrosidase depletion enhances cell-to-cell transmission of α-synuclein. *Nature communications* 5:4755. http://www.nature.com/ncomms/2014/140826/ncomms5755/full/ncomms5755.html.

26. Alvarez-Erviti, L., Y. Seow, A. H. Schapira, C. Gardiner, I. L. Sargent, M. J. A. Wood, and J. M. Cooper, 2011. Lysosomal dysfunction increases exosome-mediated alpha-synuclein release and transmission. *Neurobiology of disease* 42:360–7. http://www.pubmedcentral.nih.gov/articlerender.fcgi?artid=3107939{&}tool=pmcentrez{&}rendertype=abstract.

27. Yap, T. L., J. M. Gruschus, A. Velayati, W. Westbroek, E. Goldin, N. Moaven, E. Sidransky, and J. C. Lee, 2011. α-Synuclein Interacts with Glucocerebrosidase Providing a Molecular Link between Parkinson and Gaucher Diseases. *The Journal of Biological Chemistry* 286:28080–28088. http://www.ncbi.nlm.nih.gov/pmc/articles/PMC3151053/.

28. Yap, T. L., Z. Jiang, F. Heinrich, J. M. Gruschus, C. M. Pfefferkorn, M. Barros, J. E. Curtis, E. Sidransky, and J. C. Lee, 2015. Structural features of membrane-bound glucocerebrosidase and α-synuclein probed by neutron reflectometry and fluorescence spectroscopy. *The Journal of Biological Chemistry* 290:744–54. http://www.ncbi.nlm.nih.gov/pubmed/25429104http://www.pubmedcentral.nih.gov/articlerender.fcgi?artid=PMC4295019.

29. Mehta, A., 2006. Epidemiology and natural history of Gaucher's disease. *European Journal of Internal Medicine* 17, Supple:S2–S5. http://www.sciencedirect.com/science/article/pii/S0953620506001609http://www.sciencedirect.com/science?{_}ob=MiamiImageURL{&}{_}cid=272072{&}{_}user=4658158{&}{_}pii=S0953620506001609{&}{_}check=y{&}{_}origin=article{&}{_}zone=toolbar{&}{_}coverDate=30-Nov-2006{&}view=c{&}originContentFa.

30. Berg-Fussman, A., M. E. Grace, Y. Ioannou, and G. A. Grabowski, 1993. Human acid beta-glucosidase. N-glycosylation site occupancy and the effect of glycosylation on enzymatic activity. *The Journal of Biological Chemistry* 268:14861–14866. http://www.jbc.org/content/268/20/14861.full.pdfhttp://www.ncbi.nlm.nih.gov/pubmed/8325864http://www.jbc.org/content/268/20/14861.

31. Snead, D., and D. Eliezer, 2014. Alpha-synuclein function and dysfunction on cellular membranes. *Experimental neurobiology* 23:292–313. http://www.pubmedcentral.nih.gov/articlerender.fcgi?artid=4276801{&}tool=pmcentrez{&}rendertype=abstract.

32. Bodner, C. R., C. M. Dobson, and A. Bax, 2009. Multiple tight phospholipid-binding modes of alpha-synuclein revealed by solution NMR spectroscopy. *Journal of molecular biology* 390:775–90. http://www.pubmedcentral.nih.gov/articlerender.fcgi?artid=2709488{&}tool=pmcentrez{&}rendertype=abstract.

33. Fusco, G., A. De Simone, T. Gopinath, V. Vostrikov, M. Vendruscolo, C. M. Dobson, and G. Veglia, 2014. Direct observation of the three regions in α-synuclein that determine its membrane-bound behaviour. *Nature communications* 5:3827. http://www.nature.com/ncomms/2014/140529/ncomms4827/abs/ncomms4827.html.

34. Stefanis, L., 2012. α-Synuclein in Parkinson's disease. *Cold Spring Harbor perspectives in medicine* 2:a009399. http://www.pubmedcentral.nih.gov/articlerender.fcgi?artid=3281589{&}tool=pmcentrez{&}rendertype=abstract.

35. Vilar, M., H.-T. Chou, T. Lührs, S. K. Maji, D. Riek-Loher, R. Verel, G. Manning, H. Stahlberg, and R. Riek, 2008. The fold of alpha-synuclein fibrils. *Proceedings of the National Academy of Sciences of the United States of America* 105:8637–8642.

36. Heise, H., M. S. Celej, S. Becker, D. Riedel, A. Pelah, A. Kumar, T. M. Jovin, and M. Baldus, 2008. Solid-state NMR reveals structural differences between fibrils of wild-type and disease-related A53T mutant alpha-synuclein. *Journal of molecular biology* 380:444–50. http://www.ncbi.nlm.nih.gov/pubmed/18539297.

37. Zhou, D. H., A. J. Nieuwkoop, D. A. Berthold, G. Comellas, L. J. Sperling, M. Tang, G. J. Shah, E. J. Brea, L. R. Lemkau, and C. M. Rienstra, 2012. Solid-state NMR analysis of membrane proteins and protein aggregates by proton detected spectroscopy. *Journal of biomolecular NMR* 54:291–305. http://www.pubmedcentral.nih.gov/articlerender.fcgi?artid=3484199{&}tool=pmcentrez{&}rendertype=abstract.

38. Ecroyd, H., T. Koudelka, D. C. Thorn, D. M. Williams, G. Devlin, P. Hoffmann, and J. a. Carver, 2008. Dissociation from the oligomeric state is the rate-limiting step in fibril formation by κ-casein. *Journal of Biological Chemistry* 283:9012–9022.

39. Wang, G.-F., C. Li, and G. J. Pielak, 2010. 19F NMR studies of α-synuclein-membrane interactions. *Protein science : a publication of the Protein Society* 19:1686–91. http://www.pubmedcentral.nih.gov/articlerender.fcgi?artid=2975132{&}tool=pmcentrez{&}rendertype=abstract.

40. Lokappa, S. B., and T. S. Ulmer, 2011. Alpha-synuclein populates both elongated and broken helix states on small unilamellar vesicles. *The Journal of Biological Chemistry* 286:21450–7. http://www.jbc.org/content/286/24/21450.

41. Drescher, M., F. Godschalk, G. Veldhuis, B. D. van Rooijen, V. Subramaniam, and M. Huber, 2008. Spin-label EPR on alpha-synuclein reveals differences in the membrane binding affinity of the two antiparallel helices. *Chembiochem : a European journal of chemical biology* 9:2411–6. http://www.ncbi.nlm.nih.gov/pubmed/18821550.

42. Drescher, M., B. D. van Rooijen, G. Veldhuis, V. Subramaniam, and M. Huber, 2010. A stable lipid-induced aggregate of alpha-synuclein. *Journal of the American Chemical Society* 132:4080–2. http://www.ncbi.nlm.nih.gov/pubmed/20199073.

43. Braun, A. R., M. M. Lacy, V. C. Ducas, E. Rhoades, and J. N. Sachs, 2014. α-Synuclein-induced membrane remodeling is driven by binding affinity, partition depth, and interleaflet order asymmetry. *Journal of the American Chemical Society* 136:9962–72. http://www.ncbi.nlm.nih.gov/pubmed/24960410.

44. Galvagnion, C., A. K. Buell, G. Meisl, T. C. T. Michaels, M. Vendruscolo, T. P. J. Knowles, and C. M. Dobson, 2015. Lipid vesicles trigger α-synuclein aggregation by stimulating primary nucleation. *Nature chemical biology* 11:229–234. http://dx.doi.org/10.1038/nchembio.1750.

45. Wu, K. P., D. S. Weinstock, C. Narayanan, R. M. Levy, and J. Baum, 2009. Structural Reorganization of α-Synuclein at Low pH Observed by NMR and REMD Simulations. *Journal of Molecular Biology* 391:784–796. http://dx.doi.org/10.1016/j.jmb.2009.06.063.

46. Hoyer, W., T. Antony, D. Cherny, G. Heim, T. M. Jovin, and V. Subramaniam, 2002. Dependence of α-synuclein aggregate morphology on solution conditions. *Journal of Molecular Biology* 322:383–393.

47. Buell, A. K., C. Galvagnion, R. Gaspar, E. Sparr, M. Vendruscolo, T. P. J. Knowles, S. Linse, and C. M. Dobson, 2014. Solution conditions determine the relative importance of nucleation and growth processes in α-synuclein aggregation. *Proceedings of the National Academy of Sciences of the United States of America* 111:7671–7676. http://www.ncbi.nlm.nih.gov/pubmed/24817693.

48. Tugarinov, V., V. Kanelis, and L. E. Kay, 2006. Isotope labeling strategies for the study of high-molecular-weight proteins by solution NMR spectroscopy. *Nature Protocols* 1:749–754. http://www.nature.com/doifinder/10.1038/nprot.2006.101.

49. Larda, S. T., M. P. Bokoch, F. Evanics, and R. S. Prosser, 2012. Lysine methylation strategies for characterizing protein conformations by NMR. *Journal of biomolecular NMR* 54:199–209. http://www.ncbi.nlm.nih.gov/pubmed/22960995.

50. Takamori, S., M. Holt, K. Stenius, E. Lemke, M. Grønborg, D. Riedel, H. Urlaub, S. Schenck, B. Brügger, P. Ringler, S. Müller, B. Rammner, F. Gräter, J. Hub, B. De Groot, G. Mieskes, Y. Moriyama, J. Klingauf, H. Grubmüller, J. Heuser, F. Wieland, and R. Jahn, 2006. Molecular anatomy of a trafficking organelle. *Cell* 127:831–846. http://dx.doi.org/10.1016/j.cell.2006.10.030.

51. Mirnikjoo, B., K. Balasubramanian, and A. J. Schroit, 2009. Suicidal membrane repair regulates phosphatidylserine externalization during apoptosis. *The Journal of Biological Chemistry* 284:22512–6. http://www.pubmedcentral.nih.gov/articlerender.fcgi?artid=2755657{&}tool=pmcentrez{&}rendertype=abstract.

52. Ulmer, T. S., A. Bax, N. B. Cole, and R. L. Nussbaum, 2005. Structure and dynamics of micelle-bound human alpha-synuclein. *The Journal of Biological Chemistry* 280:9595–603. http://www.ncbi.nlm.nih.gov/pubmed/15615727.

53. Brumshtein, B., P. Salinas, B. Peterson, V. Chan, I. Silman, J. L. Sussman, P. J. Savickas, G. S. Robinson, and A. H. Futerman, 2010. Characterization of gene-activated human acid-beta-glucosidase: crystal structure, glycan composition, and internalization into macrophages. *Glycobiology* 20:24–32. http://www.ncbi.nlm.nih.gov/pubmed/19741058.

54. Rayment, I., 1997. Reductive alkylation of lysine residues to alter crystallization properties of proteins. *Methods in enzymology* 276:171–179. http://www.ncbi.nlm.nih.gov/pubmed/9048376.

55. Fabrega, S., P. Durand, P. Codogno, C. Bauvy, C. Delomenie, B. Henrissat, B. M. Martin, C. McKinney, E. I. Ginns, J.-P. Mornon, and P. Lehn, 2000. Human glucocerebrosidase: heterologous expression of active site mutants in murine null cells. *Glycobiology* 10:1217–1224. http://glycob.oxfordjournals.org/content/10/11/1217http://glycob.oxfordjournals.org/content/10/11/1217.full.pdfhttp://www.ncbi.nlm.nih.gov/pubmed/11087714http://glycob.oxfordjournals.org/content/10/11/1217.full.

56. Motabar, O., E. Goldin, W. Leister, K. Liu, N. Southall, W. Huang, J. J. Marugan, E. Sidransky, and W. Zheng, 2012. A high throughput glucocerebrosidase assay using the natural substrate glucosylceramide. *Analytical and Bioanalytical Chemistry* 402:731–739. http://www.ncbi.nlm.nih.gov/pmc/articles/PMC3351006/.

57. T. D. Goddard and D. G. Kneller. Sparky. *University of California, San Francisco* .

58. Bodner, C. R., A. S. Maltsev, C. M. Dobson, and A. Bax, 2010. Differential phospholipid binding of ??-synuclein variants implicated in Parkinson's disease revealed by solution NMR spectroscopy. *Biochemistry* 49:862–871.

59. Yap, T. L., A. Velayati, E. Sidransky, and J. C. Lee, 2013. Membrane-bound α-synuclein interacts with glucocerebrosidase and inhibits enzyme activity. *Molecular genetics and metabolism* 108:56–64. http://www.pubmedcentral.nih.gov/articlerender.fcgi?artid=3552326{&}tool=pmcentrez{&}rendertype=abstract.

60. Siebert, M., E. Sidransky, and W. Westbroek, 2014. Glucocerebrosidase is shaking up the synucleinopathies. *Brain : a journal of neurology* 137:1304–22. http://www.pubmedcentral.nih.gov/articlerender.fcgi?artid=3999712{&}tool=pmcentrez{&}rendertype=abstract.

61. Heise, H., W. Hoyer, S. Becker, O. C. Andronesi, D. Riedel, and M. Baldus, 2005. Molecular-level secondary structure, polymorphism, and dynamics of full-length alpha-synuclein fibrils studied by solid-state NMR. *Proceedings of the National Academy of Sciences of the United States of America* 102:15871–15876.

62. Comellas, G., L. R. Lemkau, D. H. Zhou, J. M. George, and C. M. Rienstra, 2012. Structural intermediates during α-synuclein fibrillogenesis on phospholipid vesicles. *Journal of the American Chemical Society* 134:5090–5099.

63. Grace, M. E., and G. A. Grabowski, 1990. Human acid beta-glucosidase: glycosylation is required for catalytic activity. *Biochemical and biophysical research communications* 168:771–777. http://www.ncbi.nlm.nih.gov/pubmed/2110456.

64. Brumshtein, B., M. R. Wormald, I. Silman, A. H. Futerman, and J. L. Sussman, 2006. Structural comparison of differently glycosylated forms of acid-beta-glucosidase, the defective enzyme in Gaucher disease. *Acta crystallographica. Section D, Biological crystallography* 62:1458–1465. http://www.ncbi.nlm.nih.gov/pubmed/17139081.

65. Kurinov, I., C. Mao, J. Irvin, and F. Uckun, 2000. X-Ray Crystallographic Analysis of Pokeweed Antiviral Protein-II after Reductive Methylation of Lysine Residues. *Biochemical and Biophysical Research Communications* 275:549–552. http://www.ncbi.nlm.nih.gov/pubmed/10964701.

66. Lund-Katz, S., J. Ibdah, J. Letizia, M. Thomas, and M. Phillips, 1988. A 13C NMR characterization of lysine residues in apolipoprotein B and their role in binding to the low density lipoprotein receptor. *J. Biol. Chem.* 263:13831–13838. http://www.jbc.org/content/263/27/13831.short.

67. Hattori, Y., K. Furuita, I. Ohki, T. Ikegami, H. Fukada, M. Shirakawa, T. Fujiwara, and C. Kojima, 2013. Utilization of lysine ^{13}C-methylation NMR for protein-protein interaction studies. *Journal of biomolecular NMR* 55:19–31. http://www.ncbi.nlm.nih.gov/pubmed/23224986.

68. Walter, T. S., C. Meier, R. Assenberg, K.-F. Au, J. Ren, A. Verma, J. E. Nettleship, R. J. Owens, D. I. Stuart, and J. M. Grimes, 2006. Lysine methylation as a routine rescue strategy for protein crystallization. *Structure (London, England: 1993)* 14:1617–1622. http://www.ncbi.nlm.nih.gov/pubmed/17098187.

69. Gerken, T. A., J. E. Jentoft, N. Jentoft, and D. G. Dearborn, 1982. Intramolecular interactions of amino groups in 13C reductively methylated hen egg-white lysozyme. *The Journal of Biological Chemistry* 257:2894–900. http://www.ncbi.nlm.nih.gov/pubmed/7061454.

70. Chavan, T. S., S. Abraham, and V. Gaponenko, 2013. Application of reductive ^{13}C-methylation of lysines to enhance the sensitivity of conventional NMR methods. *Molecules (Basel, Switzerland)* 18:7103–19. http://www.mdpi.com/1420-3049/18/6/7103.

71. Religa, T. L., R. Sprangers, and L. E. Kay, 2010. Dynamic regulation of archaeal proteasome gate opening as studied by TROSY NMR. *Science (New York, N.Y.)* 328:98–102.

72. Macnaughtan, M. A., A. M. Kane, and J. H. Prestegard, 2005. Mass spectrometry assisted assignment of NMR resonances in reductively 13C-methylated proteins. *Journal of the American Chemical Society* 127:17626–7. http://www.pubmedcentral.nih.gov/articlerender.fcgi?artid=1847388{&}tool=pmcentrez{&}rendertype=abstract.

73. Eliezer, D., E. Kutluay, R. Bussell, and G. Browne, 2001. Conformational properties of alpha-synuclein in its free and lipid-associated states. *Journal of molecular biology* 307:1061–1073.

74. Fusco, G., A. De Simone, T. Gopinath, V. Vostrikov, M. Vendruscolo, C. M. Dobson, and G. Veglia, 2014. Direct observation of the three regions in α-synuclein that determine its membrane-bound behaviour. *Nature communications* 5:3827. http://www.nature.com/ncomms/2014/140529/ncomms4827/full/ncomms4827.html.

75. Baldwin, A. J., T. P. J. Knowles, G. G. Tartaglia, A. W. Fitzpatrick, G. L. Devlin, S. L. Shammas, C. A. Waudby, M. F. Mossuto, S. Meehan, S. L. Gras, J. Christodoulou, S. J. Anthony-Cahill, P. D. Barker, M. Vendruscolo, and C. M. Dobson, 2011. Metastability of native proteins and the phenomenon of amyloid formation. *Journal of the American Chemical Society* 133:14160–14163.

76. Sidransky, E., 2005. Gaucher disease and parkinsonism. *Molecular genetics and metabolism* 84:302–4. http://www.ncbi.nlm.nih.gov/pubmed/15781189.

77. Neumann, J., J. Bras, E. Deas, S. S. O'Sullivan, L. Parkkinen, R. H. Lachmann, A. Li, J. Holton, R. Guerreiro, R. Paudel, B. Segarane, A. Singleton, A. Lees, J. Hardy, H. Houlden, T. Revesz, and N. W. Wood, 2009. Glucocerebrosidase mutations in clinical and pathologically proven Parkinson's disease. *Brain* 132:1783–1794. http://brain.oxfordjournals.org/content/132/7/1783http://brain.oxfordjournals.org/content/132/7/1783.full.pdfhttp://www.ncbi.nlm.nih.gov/pubmed/19286695http://brain.oxfordjournals.org/content/132/7/1783.full.

78. Schapira, A. H. V., and M. E. Gegg, 2013. Glucocerebrosidase in the pathogenesis and treatment of Parkinson disease. *Proceedings of the National Academy of Sciences* 110:3214–3215. http://www.pnas.org/content/110/9/3214.longhttp://www.pnas.org/content/110/9/3214http://www.ncbi.nlm.nih.gov/pubmed/23412333.